Environmental Science & Technology

pubs.acs.org/est

Article

Optimization of a NO_x and VOC Cooperative Control Strategy Based on Clean Air Benefits

Dian Ding, Jia Xing,* Shuxiao Wang,* Zhaoxin Dong, Fenfen Zhang, Shuchang Liu, and Jiming Hao

Cite This: https://doi.org/10.1021/acs.est.1c04201

Read Online

ACCESS | Metrics & More | Article Recommendations | Supporting Information

ABSTRACT: Serious ambient $PM_{2.5}$ and O_3 pollution is one of the most important environmental challenges of China, necessitating an urgent cost-effective cocontrol strategy. Herein, we introduced a novel integrated assessment system to optimize a NO_x and volatile organic compound (VOC) control strategy for the synergistic reduction of ambient $PM_{2.5}$ and O_3 pollution. Focusing on the Beijing−Tianjin−Hebei cities and their surrounding regions, which are experiencing the most serious $PM_{2.5}$ and O_3 pollution in China, we found that NO_x emission reduction (64−81%) is essential to attain the air quality standard no matter how much VOC emission is reduced. However, the synergistic VOC control is strongly recommended considering its substantially human health and crop production benefits, which are estimated up to 163 ($PM_{2.5}$-related) and 101 (O_3-related) billion CHY during the reduction of considerable emissions. Notably, such benefits will be greatly reduced if the synergistic VOC reduction is delayed. This study also highlights the necessity of simultaneous VOC and NO_x emission control in winter while enhancing the NO_x control in the summer, which is contrary to the current control strategy adopted in China. These findings point out the right pathways for future policy making on comitigating $PM_{2.5}$ and O_3 pollution in China and other countries.

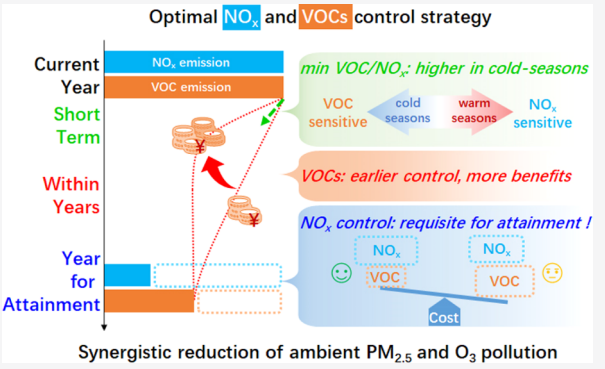

KEYWORDS: *$PM_{2.5}$, O_3, synergistic control pathway, response surface model, integrated assessment*

INTRODUCTION

Attaining the air quality specified by the "Beautiful China" strategy[1] has become the most urgent and important task for air management in China. Although the air quality in China has significantly improved since the implementation of the Air Pollution Prevention and Control Action Plan from 2013 to 2017,[2] the concentration specified by the National Ambient Air Quality Standard (NAAQS) for annual fine particulate matter with an aerodynamic diameter ≤2.5 μm ($PM_{2.5}$) of 35 $\mu g/m^3$ (GB 3095-2012) is still distant,[3] especially in the Beijing−Tianjin−Hebei (BTH) region (64 $\mu g/m^3$ in 2017).[4] Furthermore, ozone (O_3) pollution has become increasingly prominent in 338 Chinese cities, 32.3% of which exceeded the national standard (>160 $\mu g/m^3$) in 2017. Additionally, the average 90th percentiles of the daily maximum 8 h average (MDA8) O_3 concentration increased by 24.5% in BTH from 2013 to 2017.[1] Therefore, an integrated control strategy needs to be urgently optimized to achieve both O_3 and $PM_{2.5}$ air quality improvements in China.

Previous studies have mostly focused on revealing the complex photochemical interactions[5−8] between $PM_{2.5}$ and O_3, which raised concerns about the simultaneous reduction of both pollutants. From the environmental management aspect, the crucial question about how to present the collaborative control measures for addressing the couplings between $PM_{2.5}$ and O_3 is still unanswered. The emission of precursors is surely the most significant factor affecting $PM_{2.5}$ and O_3 concentrations, as demonstrated by the long-term trend of O_3 in Beijing,[9] which is completely attributed to the changes in NO_x and volatile organic compound (VOC) emissions. Another challenge comprises the optimization of NO_x and VOC precursor emissions to effectively reduce $PM_{2.5}$ and O_3 concentrations, particularly for O_3 as it strongly depends on the relative changes of NO_x and VOC in addition to the absolute changes.[10] Some studies have emphasized the importance of VOC reduction in urban areas, which usually exhibit strong VOC sensitivity.[11−13] Additionally, another study determined that NO_x reduction can also decrease the peak O_3 levels due to the NO_x-sensitive regime during peak O_3 hours in the metropolitan region.[14,15] The short-term control strategy can be analyzed based on the current O_3 formation sensitivity in the region. However, to substantially reduce O_3 concentrations, the NO_x emissions as well as, or instead of,

Received: June 24, 2021
Revised: December 3, 2021
Accepted: December 14, 2021

VOCs need to be controlled,[16] which was also verified by the O_3 pollution control in the United States. This implies that the short-term optimal control strategy is likely to be inconsistent with the long-term control demand. Further, although they may be effective in reducing O_3 in short-term, the unified and fixed emission control ratios of VOCs and NO_x with a wide range that have been proposed by many studies[13,17−19] are unrealistic and neglect the discrepancies across the regions and seasons as well as the future dynamic changes in atmospheric chemistry with emission control. Thus, the design of a reasonable control pathway by combining the control requirements of different time periods is problematic. Only a few studies have analyzed the control path combined with the cost optimization.[20] However, due to the limitations of existing methods, optimizing the control strategy directly based on the pollutant's concentration changes is difficult. This may be the reason why few previous studies have considered air quality attainment and environmental benefits, especially health benefits. To address the abovementioned limitations, this study aimed to answer the crucial question of how to wisely optimize NO_x and VOC controls to attain the air quality standards and maximize the associated health and ecological benefits in China.

Herein, we developed a novel integrated assessment system to optimize the NO_x and VOC control strategies for the synergistic reduction of ambient $PM_{2.5}$ and O_3 pollution. The BTH and surrounding regions are currently experiencing the most serious $PM_{2.5}$ and O_3 pollution in China. Therefore, the target region of this study comprises the 2+26 cities in the BTH and surrounding regions (the 2+26 cities were first mentioned in the 2017 Air Pollution Prevention and Management Plan, which was released by the China Ministry of Environmental Protection, including Beijing, Tianjin, and 26 surrounding cities; details can be found in Table S1 and Figure S1). The novel integrated assessment system combines a detailed bottom-up emission inventory, an emission-concentration response surface model (RSM), a least-cost optimization model, and an associated benefit assessment model. This system affords high efficiency in predicting the real-time response of air quality to emission changes, and the simultaneous estimation of the associated cost and benefit enables the selection of an optimized control strategy from numerous options. Details of the methods and data are provided in the following sections.

METHODS

Model Simulation Setups. This study adopted the Community Multiscale Air Quality (CMAQ) model v5.2[21] to simulate the $PM_{2.5}$ and O_3 concentrations. One-way and double-nesting simulation domains were employed (Figure S1). The parent domain covers mainland China and the portions of the surrounding countries with a grid resolution of 27 km × 27 km. The nested domain covers the BTH and surrounding regions with a grid resolution of 9 km × 9 km. Furthermore, we employed Carbon Bond 6[22] gas-phase chemistry and the AERO6 aerosol module.[23] The anthropogenic emission data of BTH and surrounding regions were obtained from the 2016 Multiresolution emission inventory for China with 0.1° × 0.1° resolution[24] (data from 2017 were unavailable at the beginning of the simulation). Figure S2 shows the major air pollutant emissions of the 2+26 cities. Biogenic emissions were generated using the Model for Emissions of Gases and Aerosols from Nature version 2.04.[25] A 5 day spin-up was performed to reduce the influence of initial conditions. The meteorology fields for CMAQ were generated using the Weather Research and Forecasting model (WRF) version 3.8.[26] The detailed configuration is present in a previous study.[2]

The simulation period was the entire year of 2017. We compared the meteorological parameters simulated by the WRF model to the observational data downloaded from the National Climatic Data Center and compared the hourly $PM_{2.5}$ and O_3 concentrations simulated by CMAQ with the observational data obtained from the China National Environmental Monitoring Centre (http://106.37.208.233:20035/). Figure S3 shows the locations of the state-controlled air quality observational sites in the 2+26 cities. Generally, the model well reproduced the meteorological conditions and air pollutant concentrations in 2017. Details of the model evaluation results are provided in Supporting Information Note 1 (Tables S2−S6 and Figures S4 and S5).

Development of the Emission-Concentration Response Models. RSM technology affords an efficient way to quantify the response of the concentration to emission changes by forming a "real-time" relationship between air pollution and precursor emissions based on the large amounts' simulation of chemical transport models.[27,28] To extend the applicability of estimating the response of the concentration to emission changes in city clusters, the extended RSM (ERSM) was applied. In ERSM, the response of $PM_{2.5}$ and O_3 concentrations is divided into local chemical generation and regional transportation and is subsequently integrated to derive the total $PM_{2.5}$ concentration in the target region.[29,30] Additionally, this model simultaneously addresses the indirect effects of interaction among regions according to regional emission changes.[31] However, extremely high computational costs limit the application of the ERSM. In this study, to establish a multiregional prediction system for multiple cities, we developed pf-ERSM by combining RSM with polynomial functions (pf-RSM)[16] and ERSM. A detailed description of the polynomial functions is provided in Supporting Information Note 2.

Overall, 28 target regions in the inner modeling domain were defined (Figure S1b), i.e., the 2+26 cities. Then, 686 emission control scenarios (Table S7) were simulated to establish the pf-ERSM prediction system according to the polynomial function form, including (1) 1 CMAQ base case; (2) 21 emission control scenarios for sequentially controlling NO_x, SO_2, NH_3, and VOCs in each region (588 scenarios in total); (3) two emission control scenarios to sequentially control the primary $PM_{2.5}$ emission ratio in each region, 56 scenarios in total; and (4) 41 emission control scenarios for the total emission of NO_x, SO_2, NH_3, and VOCs over the entire region. The first three sets of scenarios (645 in total) were used to establish the response surfaces of local chemical generation of single-region and multiregional transportations. The overall regional control scenarios combined with the base case (42 in total) were considered to supplement the calculation of indirect effects. The prediction performance with different training samples for predicting $PM_{2.5}$ and O_3 has been previously discussed.[32] Samples were generated using a Hammersley quasi-random sequence sample with additional marginal processing,[28] sampling emission ratios between 0 and 2 (baseline = 1). Totally, 140 control variables were included in the predicted system, including five precursors in the 2+26 cities. According to the technical regulation for ambient air

https://doi.org/10.1021/acs.est.1c04201
Environ. Sci. Technol. XXXX, XXX, XXX−XXX

quality assessment in China (HJ663-2013), the air quality of a city meets the air quality standard or not is judged based on the average of the national-controlled air quality observational sites. Thus, the response variables comprised the average $PM_{2.5}$ and O_3 concentrations of the grid cells, which contain monitoring sites (Figure S3).

Validation of the Model's Prediction Performance. The pf-RSM system for simultaneous emission changes in the entire region was verified using the leave-one-out method. Table S8 shows the normalized bias of the pf-RSM predicted $PM_{2.5}$ and O_3 compared to the simulated result by CMAQ. The correlation coefficients were larger than 0.99. For the predicted $PM_{2.5}$ response, the mean normalized bias (MNB) was between −2.3 and 2.7%, and the normalized mean bias (NMB) was between −3.2 and 3.9%. For the predicted O_3 response, the MNB and NMB were between −0.5 and 0.4%. This implies that the pf-RSM prediction and the simulation well agree.

Then, the performance of the pf-ERSM prediction system for multiple regions was examined using out-of-sample validation. Overall, 18 independent scenarios were generated wherein the 140 control variables were simultaneously changing, including nine cases generated with average emission ratios of 0.15, 0.25, 0.35, 0.45, 0.55, 0.65, 0.75, 0.85, and 0.95 and variance of 0.05 using Latin hypercube sampling (LHS) to evaluate the prediction accuracy of large-range emission changes and nine cases randomly generated by LHS with emission ratios from 0 to 1. Figure S6 shows the emission ratios for the 18 out-of-sample validations. Figure S7 shows the scatter plot of $PM_{2.5}$ and O_3 concentrations predicted by pf-ERSM and simulated by CMAQ. The $PM_{2.5}$ verification results for each city showed that MNB was −0.3 to 2.8%, NMB was 0.1−2.7%, mean normalized error (MNE) was 0.7−3.1%, normalized mean error (NME) was 0.7−2.9%, and the correlation coefficient was larger than 0.99. The O_3 verification results for each city showed that MNB was −1.1 to 1.3%, NMB was −1.1 to 1.3%, MNE was 0.3−1.6%, NME was 0.3−1.6%, and the correlation coefficient was >0.90. The verification results denoted that the pf-ERSM predicted system is reliable.

We further tested whether the predicted two-dimensional (2-D) isopleth obtained using the pf-ERSM well matches the pf-RSM prediction when the overall regional precursor emission ratio continuously changes from 0 to 1. Figures S8 and S9 show the comparison of the 2-D isopleths of $PM_{2.5}$ and O_3 concentrations in Beijing according to the simultaneous changes in precursor emissions in 2+26 cities derived using the pf-RSM and pf-ERSM techniques. The results indicate the reliability of pf-ERSM during the continuous variation of the precursor emissions, and it can be used to evaluate the change in the pollutant concentration under different control scenarios.

Furthermore, we performed data fusion by combining the simulation and observation data to reduce the uncertainty introduced by the simulation. The prediction concentrations adjusted by applying the relative changes in simulation to the observations in the base year were used in the following analysis.

Estimation of Costs and Benefits. The control costs were estimated using marginal abatement cost curves. The marginal abatement cost curves of NO_x and VOCs in the target region were obtained from Xing et al.[33] The cost is highly related to the emission reduction ratio of precursors. Thus, the discussion of emission reduction ratios represents the comparison of costs. Moreover, the optimization herein was not based on the cost estimation of specific control measures.

Benefits assessment comprised the impact analysis of human health and crop yields. Derived from epidemiological studies, the excess mortality related to air pollution can be calculated using the hazard risk model method[34]

$$M = P \times I \times (1 - 1/\mathrm{HR}) \quad (1)$$

where M is the mortality that is attributable to ambient air pollution, I is the average annual mortality rate, P is the population, and HR is the hazard risk.

Furthermore, the health effects due to $PM_{2.5}$ exposure were estimated by adopting a global exposure mortality model (GEMM).[35] The HR in the GEMM model was calculated using eq 2

$$\mathrm{GEMM}(z) = \exp\{\theta \log(z/\alpha + 1) / (1 + \exp\{-(z-\mu)/\nu\})\} \quad (2)$$

where $z = \max(0, PM_{2.5}\text{-}2.4\ \mu g/m^3)$, and θ, α, μ, and ν are unknown parameters introduced in the previous study.[35] GEMM parameters including the Chinese Male Cohort study[36] were selected. Using the GEMM model, we calculated the mortality due to noncommunicable diseases and lower respiratory infection causes. The annual Chinese national cause-specified mortality rates in 2017 were obtained from the GBD results tool.[37] Additionally, the city-level population in 2017 was obtained from China's statistical yearbooks.[38] To estimate the health effects due to O_3 exposure, we referred to Turner et al.[39] They suggested the positive associations between summer O_3 and all-cause mortality [HR per 10 ppb, 1.02; 95% confidence interval (CI), 1.01−1.03]. Then, we monetized the health effects to afford economic benefits by multiplying by the value of statistical life (VSL). A VSL of 5.24 (95% CI, 3.51−6.98) million CNY was estimated through a choice experiment survey using the willingness-to-pay method.[40]

O_3 pollution can significantly affect the crop yield. In China, wheat, maize, and rice are major crops. In 2+26 cities, the total yields of wheat, maize, and rice in 2017 were 42 933, 45 492, and 1604 kt, respectively (Table S9). AOT40 is an index that is widely used to protect vegetation against O_3;[41] it is the sum of hourly O_3 concentrations higher than 40 ppb over 12 h (8:00−19:59) during the crop growing season. The accumulation time window of winter wheat, maize, and rice is April 1−June 15,[41] June 22−September 23,[42] and July 1−September 30.[43] We adopted the recent exposure response functions[43] of relative yield (RY) and AOT40 for winter wheat, maize, and rice (Table S10). Crop production losses (CPLs) were calculated as follows

$$\mathrm{CPL} = \mathrm{CP} \times \mathrm{RYL}/(1 - \mathrm{RYL}) \quad (3)$$

where CP is the crop production and RYL is the RY loss. For a crop corresponding to multiple exposure response functions, we calculated the average. The economic losses were calculated based on market prices in China, which were obtained from the Food and Agriculture Organization of the United Nations (https://fpma.apps.fao.org/giews/food-prices/tool/public/#/dataset/domestic). The average costs of wheat, maize, and rice in China were ∼2528, 1676, and 4331 CHY/t in 2017, respectively.

https://doi.org/10.1021/acs.est.1c04201
Environ. Sci. Technol. XXXX, XXX, XXX−XXX

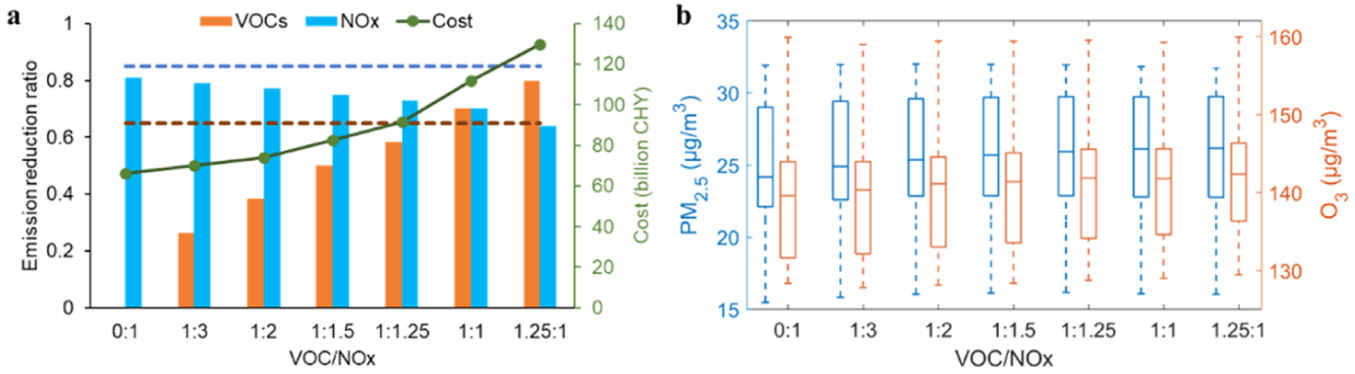

Figure 1. Cost and air quality impacts of various VOC/NO_x control ratios. (a) Emission reduction requirements of NO_x and VOCs to ensure that $PM_{2.5}$ and O_3 concentrations in 2+26 cities meet the air quality standards under the restrictions of different VOC/NO_x reduction ratios. The blue dotted line is the upper limit of the NO_x reduction ratio in 2035. The orange dotted line is the upper limit of the VOC reduction ratio in 2035. The maximum reduction ratio of NO_x and VOCs was set as ~85 and 65%, respectively, after considering all potential controls.[33] The green line denotes the cost of NO_x and VOC control. (b) Predicted $PM_{2.5}$ and O_3 concentrations of the 2+26 cities under different VOC/NO_x reduction ratios (error bars represent the concentrations range in the 2+26 cities).

RESULTS

Achieving Air Quality Standards Requires Stricter Control of NO_x than VOCs. The observed annual concentrations of $PM_{2.5}$ and O_3 in the 2+26 cities ranged from 57 to 86 and 178 to 216 $\mu g/m^3$, respectively, in 2017. The concentrations of both pollutants far exceed the NAAQS of China (GB 3095-2012, wherein the annual $PM_{2.5}$ concentration is 35 $\mu g/m^3$ and the annual 90th percentile MDA8 O_3 concentration is 160 $\mu g/m^3$ for Grade II regions), which implies that near-maximum controls are required for all of the precursors. This is demonstrated in our previous study[3], which suggests that the aggressive implementation of low carbon energy policies with end-of-pipe control at the maximum feasible reduction level (noted as the CBE, cobenefit energy scenario) is necessary to meet the air quality standard in the 2+26 cities (detailed in Table S11). However, the nonlinear $PM_{2.5}$ and O_3 responses to NO_x and VOC emissions cause significant variation in the control efficiency of NO_x and VOCs for air pollution reduction. Here, we compared the requirements of NO_x and VOC controls that can make both $PM_{2.5}$ and O_3 meet the standards in the 2+26 cities (except O_3 in Taiyuan, Zibo, Zhengzhou, and Tangshan, which required outside emissions control; this is explained in Supporting Information Note 3 and shown in Figure S10). We changed the combination of NO_x and VOC emission reduction ratios in the 2+26 cities and applied the same reductions for other pollutants (i.e., primary $PM_{2.5}$ was reduced by 65−87%, SO_2 was reduced by 49−85%, and NH_3 was reduced by up to 29%) and outer regions as those in the CBE scenario (Figure S11 shows the concentration reductions in the 2+26 cities due to outer-regional control). The results suggest that the NAAQS can be attained if the NO_x emissions are reduced by ~81% relative to 2017, even without VOC control (Figure 1a). If the VOC controls are increased from 26 to 80% (Figure 1a), the required minimum NO_x emission reduction ratio ensuring $PM_{2.5}$ and O_3 concentration attainment (Figure 1b) in the 2+26 cities can decrease from 79 to 64%. However, the associated cost also significantly increases from 66 to 130 billion CHY along with the growth of VOC/NO_x ratios from 0:1 (no VOC control) to 1.25:1 (VOC control is 1.25 times the NO_x control). In other words, the increase in VOC reductions of 80% can slightly reduce the requirement of NO_x reductions of 17% but with an extra 96% associated cost (63 billion CHY). In reality, however, the adoption of a specific control strategy needs to comprehensively consider the technical feasibility, economic rationality, regional adaptability, and implementation possibilities; therefore, achieving maximum NO_x controls will take a sufficiently long time. Therefore, the optimization of NO_x and VOC controls needs to be dynamically considered in the future.

Prompt Synergistic Control of NO_x and VOCs Has Great Benefits. Since a large proportion of precursor emissions need to be reduced, it may take more than 10 years to attain the NAAQS.[1] If VOC emissions are not controlled, the limited NO_x control in the first few years might enhance the O_3 pollution,[30,44] which occurred in some Chinese cities during 2013−2019.[13,45] Therefore, different NO_x and VOC control pathways could afford different benefits even if the final air quality targets are the same, i.e., attaining NAAQS.

To attain the NAAQS for both $PM_{2.5}$ and O_3, the emission reduction ratios of NO_x and VOCs need to reach 75 and 50%, respectively, in 2035 (close to the CBE prediction with a VOC/NO_x reduction ratio of ~0.51). Accordingly, NO_x emissions were assumed to annually decrease by 7.4%. Primary $PM_{2.5}$, SO_2, and NH_3 emissions annually decreased by 5.6−10.7, 3.7−9.9, and −0.3 to 1.9%, respectively, for the 2+26 cities according to the CBE scenario. Under this assumption, we compared the associated benefits under different VOC emission reduction rates, that is, VOC emissions were reduced in different periods. As shown in Figure 2a, we designed 14 control scenarios with different VOC control paces, which subsequently afforded a 50% reduction in VOC emissions during different periods (i.e., 5−18 years). For each scenario, the annual emission reduction rate was the same during the emission control period. Furthermore, since the final emission reduction of VOC in each scenario was the same, we assumed that the economic costs of different paths do not significantly differ. Note that the emergence of new control techniques and the control cost may differ in the future. Most likely, the control cost will reduce with technology innovation in the future.

All scenarios afforded the same air quality target in the last year; however, the air quality and related benefits were considerably different during the previous years. Compared to the attainment of 50% VOC reduction over 18 years, the prompt synergistic control of NO_x and VOCs has great

https://doi.org/10.1021/acs.est.1c04201
Environ. Sci. Technol. XXXX, XXX, XXX−XXX

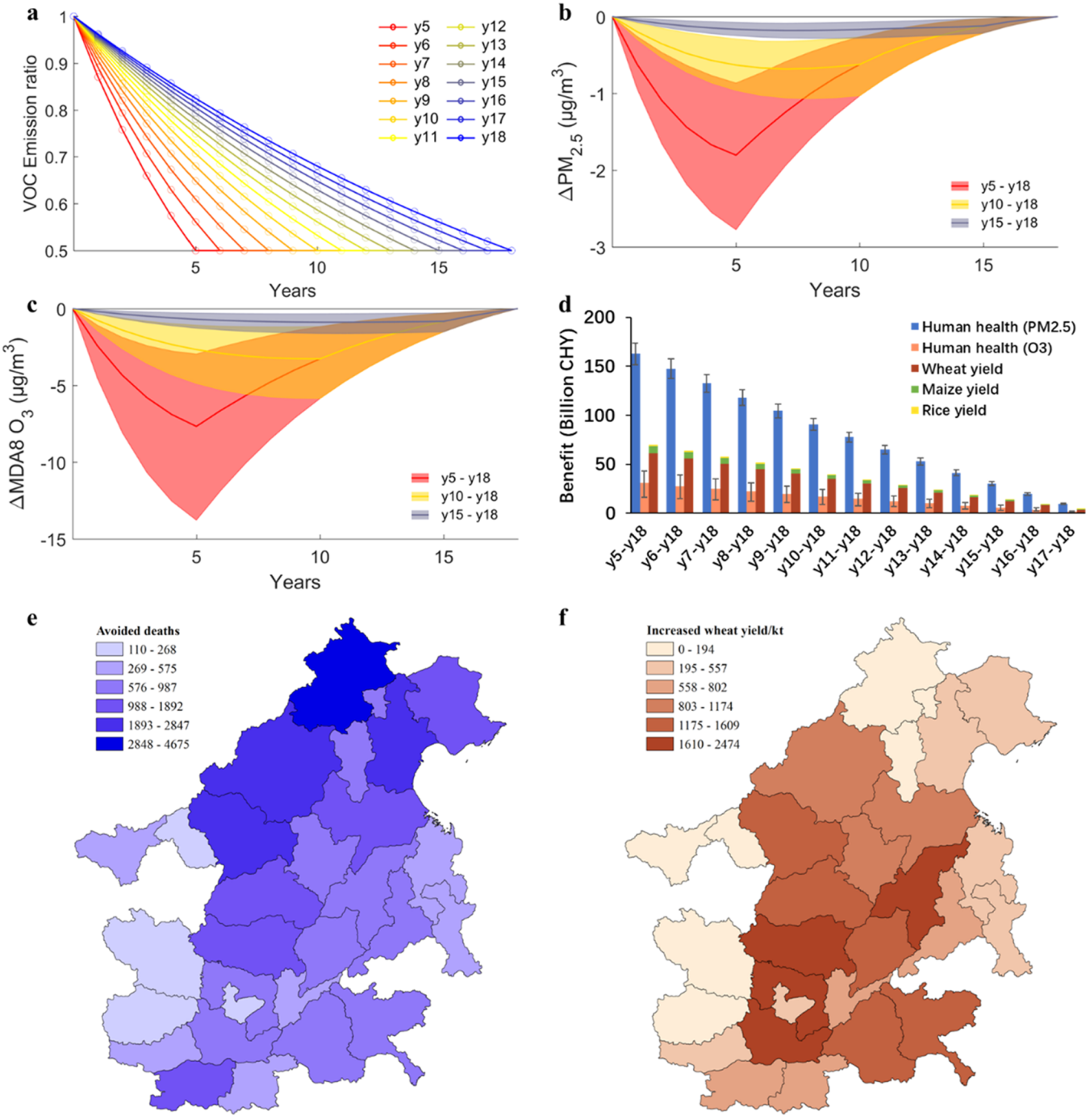

Figure 2. Pollutant concentration under different emission reduction paths and related benefit estimation of cooperative VOC emission reduction. (a) Different designed emission control paths of VOCs with a certain reduction amount (50%) but will be completed within 5−18 years (denoted as y5, y6, ..., and y18). (b) Impact of VOC emission reduction completed in the 5, 10, and 15 years on the annual $PM_{2.5}$ concentration compared to the emission reduction completed in 18 years. The solid line and shadow represent the median concentration change and its ranges in the 2+26 cities. (c) Same as (b) but for the 90th MDA8 O_3 concentration. (d) Additional $PM_{2.5}$- and O_3-related health benefits, and O_3-related crop yield benefits of control path y5−y17 relative to that of y18. (e) Total avoided $PM_{2.5}$-related deaths due to the completion of VOC reduction in 5 years than in 18 years throughout the entire pathway. (f) Total avoided wheat yield losses due to the completion of VOC reduction in 5 years than in 18 years throughout the entire pathway.

benefits. Extra air quality benefits are afforded with more aggressive and faster VOC emission control. Figure 2b,c shows the additional reduction of the annual $PM_{2.5}$ and 90th MDA8 O_3 concentrations in the entire control period with faster VOC emission control to those under uniform VOC reduction over 18 years. Taking the VOC reduction achieved within 5, 10, and 15 years as an example, the extra reduction of ambient $PM_{2.5}$ and O_3 was up to 2.8 and 13.8, 1.1 and 5.9, and 0.3 and 1.6 $\mu g/m^3$, respectively, compared to the VOC reduction achieved in 18 years. Apparently, largely controlling VOCs in the early stage can ensure the effectiveness of NO_x control in reducing $PM_{2.5}$ and O_3. Such reduced $PM_{2.5}$ and O_3 concentrations stemming from aggressive VOC control strategies can afford additional benefits by mitigating their adverse influences on

https://doi.org/10.1021/acs.est.1c04201
Environ. Sci. Technol. XXXX, XXX, XXX−XXX

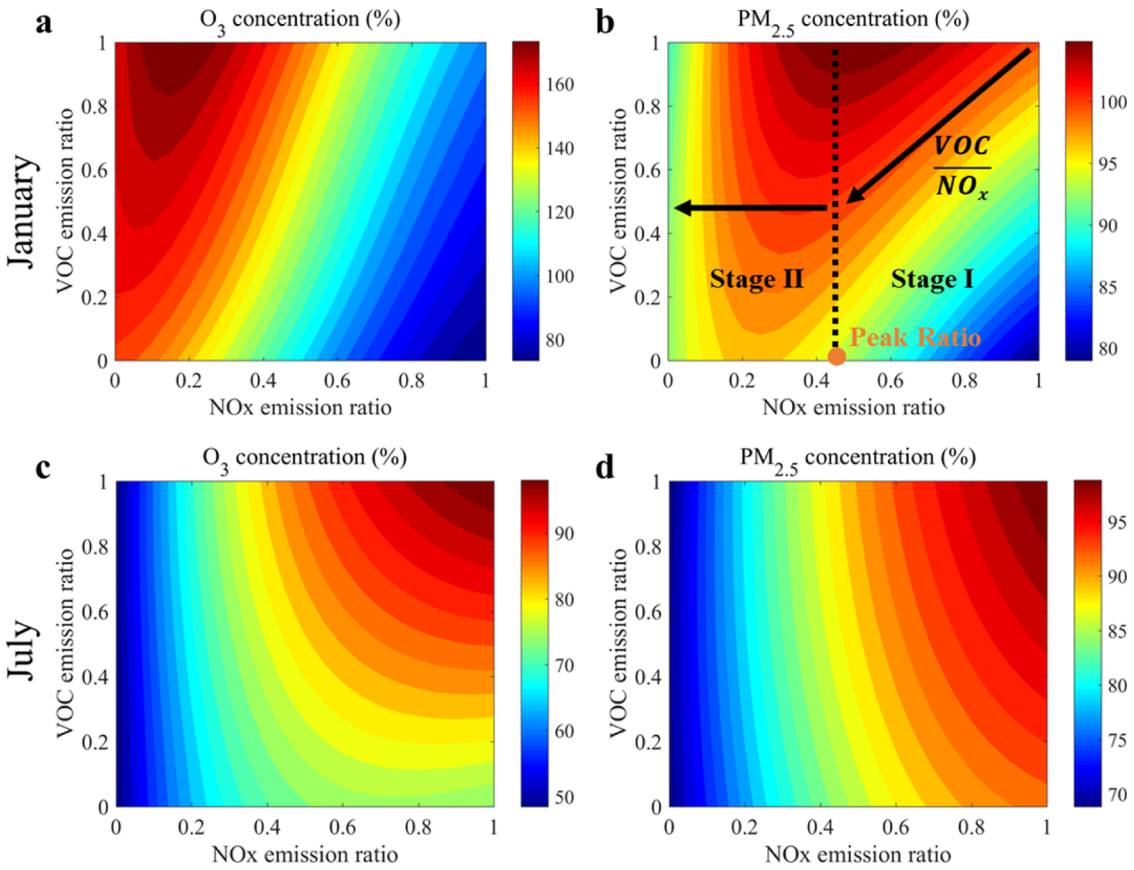

Figure 3. Isopleths of pollutant concentrations in Beijing according to the emission changes of NO_x and VOCs in the 2+26 cities. (a) O_3 and (b) $PM_{2.5}$ concentration changes according to the NO_x and VOC emission changes in January. (c) O_3 and (d) $PM_{2.5}$ concentration changes according to the NO_x and VOC emission changes in July. The color represents the percentage change in the concentration relative to the baseline. The O_3 concentration is the monthly average MDA8 O_3 concentration in Beijing; the $PM_{2.5}$ concentration is the monthly average of the 24 h average in Beijing. Note that the concentrations are averages of all monitor stations in Beijing including both urban and suburban stations (Figure S20). Urban sites with higher NO_x emission intensities usually exhibit higher sensitivity to VOC reduction than suburbs.[54,55]

human health and ecosystems (Figure 2d). The total estimated $PM_{2.5}$-related deaths under 13 different paths of faster VOC control were lower by 1836−31 095 cases than those under uniform VOC reduction over 18 years. The largest benefit was the scenario where VOC emission reductions could be achieved within 5 years, which yielded 99−4020 cases/year and 31 095 avoided deaths (95% CI, 28.9−33.2), particularly in the northern 2+26 cities (Figure 2e). These avoidable $PM_{2.5}$-related deaths are large enough to be considered when designing the control pathway in the future. The total estimated O_3-related deaths under 13 different paths of faster VOC control were lower by 362−5879 cases than those under uniform VOC reduction over 18 years. Additionally, reduced O_3 will prevent yield losses of 1566−24 342 kt of wheat, 271−4349 kt of maize, and 19−291 kt of rice. Wheat is more sensitive to O_3 than other crops, and it accounts for a large proportion of North China's grain output. Taking the reduction in wheat yield loss as an example, a 50% VOC emission reduction within 5 years may prevent losses of 102−3021 kt/year, increasing the total wheat yield by 24342 kt, particularly in the southern part of the 2+26 cities (Figure 2f). This indicates that VOC reduction is beneficial for O_3 control during the crop growing season, which is mostly in the VOC-sensitive regime, and affords additional benefits for reducing additional O_3 during the pathway.

We compared the monetized health and ecological benefits associated with the extra air quality improvements in Figure 2d. Even when the emission reductions are completed 1 year ahead of schedule, large benefits can be obtained, including 9.6 billion CHY for $PM_{2.5}$-related health benefits, 1.9 billion CHY for O_3-related health benefits, and 4.5 billion CHY for ecological benefits. The benefits will increase with the faster implementation of the VOC emission reductions. If a radical control strategy is achieved within 5 years, additional benefits can be obtained, including health benefits of 163 billion CHY related to $PM_{2.5}$ concentration reduction, health benefits of 31 billion CHY related to O_3 concentration reduction, and 61.5, 7.3, and 1.3 billion CHY benefits due to the prevention of wheat, maize, and rice production losses related to O_3 exposure, respectively. Different VOC control paths (VOC/NO_x ratio ranging from 0.5 to 1.7) have more significant impacts on O_3 pollution; however, the associated reduction in the $PM_{2.5}$ concentration affords large unexpected health benefits. Furthermore, we performed a similar comparison between synergistic controls and only the NO_x control (81%). Precursor emissions are assumed to decrease in equal proportions over 18 years. The extra benefits of synergistic NO_x and VOC control are estimated to be 107 billion CHY, including health benefits of 29.7 (95% CI, 21.2−38.1) billion CHY attributed to $PM_{2.5}$ reduction, 22.7 (95% CI, 11.5−32.3) billion CHY attributed to O_3 reduction, and 72.0, 4.4, and 1.2

https://doi.org/10.1021/acs.est.1c04201
Environ. Sci. Technol. XXXX, XXX, XXX−XXX

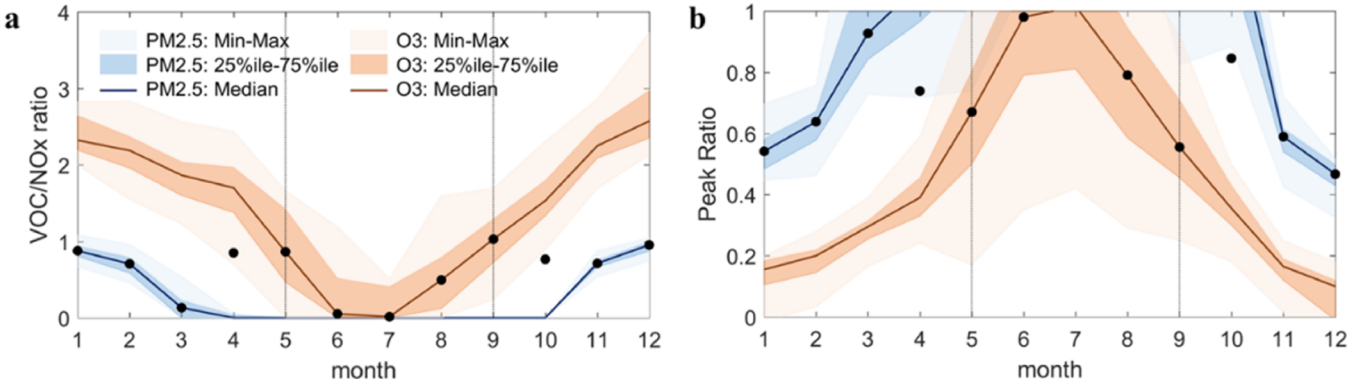

Figure 4. Monthly NO_x and VOC emission reduction requirements. (a) VOC/NO_x reduction ratio to prevent increases in $PM_{2.5}$ and O_3 concentrations. The black dots represent the suggested ratio (with the ratio for May−September from O_3, ratios for January−February and November−December from $PM_{2.5}$, and ratios for the transition months of April and October from the average of both). (b) Variation of peak ratios (NO_x emission ratio at the peak pollutant concentrations under the baseline VOC emissions) indicates the degree of NO_x emission reduction required to transform from VOC- to NO_x-sensitive. The black dots represent the suggested ratio (with the ratio for May−September from O_3, ratios for January−February and November−December from $PM_{2.5}$, and ratios for the transition months of April and October from the average of both).

billion CHY due to the prevention of wheat, maize, and rice production losses, respectively. The benefits are significantly higher than the cost of VOC control (16.1 billion CHY). That is, the synergistic NO_x and VOC control will provide more substantial benefits than only NO_x control.

Optimal NO_x and VOC Control Strategies Vary with Season. Previous studies have focused on NO_x and VOC control targeting O_3 reduction. High O_3 concentrations are present in the summer in North China. In the winter in North China, however, the O_3 concentration is generally far below the NAAQS, while the $PM_{2.5}$ concentrations frequently exceed the NAAQS. Moreover, the $PM_{2.5}$ concentration is significantly influenced by the NO_x and VOC control ratio, as demonstrated by the monthly variations of $PM_{2.5}$ and O_3 concentrations in the 2+26 cities to changes in NO_x and VOC emissions across a year. Note that the basic assumption of the study is joint control over 2+26 cities; thus, the discussion on O_3 formation sensitivity is based on the emission changes over the entire region (detailed explanation is provided in Supporting Information Note 4, Figures S12−S14).

First, we describe the typical response characteristics in the winter and summer. Although the response characteristics of each city are different, here, we aim to highlight the differences between seasons. Since all cities exhibited similar seasonal differences, here, we considered Beijing's results as an example. Figure 3 shows the isopleths of the monthly average $PM_{2.5}$ and monthly average MDA8 O_3 according to the NO_x and VOC emission changes in January and July. In the winter (i.e., January), O_3 formation is in a strong VOC-sensitive regime, as NO_x emission reduction increases O_3 by up to 77% when NO_x is reduced by 85% (see Figure 3a). This VOC-sensitive regime was proven by the COVID-19 lockdown during January−March in 2020.[46−48] Fortunately, the O_3 concentration is very low in winter. For example, the monthly average MDA8 O_3 in Beijing was 43 $\mu g/m^3$ in January 2017. Regardless of the VOC and NO_x combination chosen, the MDA8 O_3 did not exceed the WHO guidelines (100 $\mu g/m^3$ for the daily value). Therefore, the control measures in the winter should focus on $PM_{2.5}$ control. If only NO_x is controlled and VOCs are not controlled, the emission change may increase the atmospheric oxidation and considerably affect the formation of secondary $PM_{2.5}$, such as secondary organic matter (OM).[49−52] Because of the strong VOC-sensitive regime in winter, $PM_{2.5}$ will increase by up to 6% when only NO_x is reduced by 50%, and this adverse effect will continue until NO_x reduction reaches 80% (Figure 3b). Such nonlinearities are mostly derived from the changes in NO_3^- and OM, which are the two main components in $PM_{2.5}$ (Supporting Information Note 5, Figure S15a,b). The increase of the $PM_{2.5}$ concentration can be prevented when the VOC/NO_x reduction ratio is 0.87. In July, both $PM_{2.5}$ and O_3 need to be simultaneously controlled since both $PM_{2.5}$ and MDA8 O_3 are considerably high (e.g., 52 and 170 $\mu g/m^3$ in Beijing, respectively, which are higher than the standards). The NO_x-sensitive regime affords a positive sensitivity of O_3 to NO_x (Figure 3c); thus, the zero-out regional NO_x emissions can reduce the O_3 concentration by 51%. In comparison, zero-out VOC emissions only reduce the O_3 concentration by 26%. Apparently, the substantially reduction of NO_x emissions in the summer is more effective for the future control of O_3 than that of VOCs, partly due to the uncontrollably high biogenic VOC emissions (Figure S16). $PM_{2.5}$ also exhibits positive sensitivity to NO_x emissions (Figure 3d) due to the increased sensitivity of NO_3^- and OM to NO_x reduction (Supporting Information Note 5, Figure S15c,d) because the $PM_{2.5}$ concentration can decrease up to 31% by zeroing out NO_x, and this value is considerably higher than that under the zero-out VOC emissions (8%). The effectiveness of controlling NO_x in the summer agrees with a recent study.[53] The isopleths of $PM_{2.5}$ and O_3 concentrations in other cities are shown in Figures S17−S19.

Here, we define the simultaneous VOC/NO_x reduction ratio as the minimal VOC/NO_x ratio that can prevent the increase in $PM_{2.5}$ and O_3 due to the NO_x reduction under a VOC-sensitive regime (Figure 3b). We performed the same analysis for all of the cities and obtained the following results. The value significantly varies across a year (Figure 4a), with high values in cold seasons and low values in warm seasons. The synergistic control of $PM_{2.5}$ and O_3 reduces the annual average $PM_{2.5}$ and the 90th MDA8 O_3 concentrations and reduces the nonattainment days for both $PM_{2.5}$ and O_3 (i.e., reducing the short-term peak values of $PM_{2.5}$ and O_3). In terms of the monthly concentration variation of the two pollutants (Figure S21a,b), VOC does not need to be excessively controlled to lower the O_3 in the winter. The VOC/NO_x reduction ratios

https://doi.org/10.1021/acs.est.1c04201
Environ. Sci. Technol. XXXX, XXX, XXX−XXX

targeting the $PM_{2.5}$ decrease are 0.88 (min−max value of the 2+26 cities, 0.67−1.1), 0.71 (0.46−0.96), 0.71 (0.36−1.04), and 0.95 (0.74−1.19) in January, February, November, and December, respectively. The warm season (i.e., May−September) is the key season for the simultaneous control of O_3 and $PM_{2.5}$; therefore, adopting the VOC/NO_x reduction ratio targeting the lower O_3 peak is essential. The VOC/NO_x reduction ratios were 0.86 (0−3.54), 0.05 (0−1.79), 0.02 (0−1.65), 0.50 (0−2.15), and 1.03 (0.23−2.20) for May−September, respectively. In addition to the large demand for VOC emission reduction in cities close to the border of the region (Figures S13b and S14c), Tianjin, Shijiazhuang, Xingtai, Handan, Anyang, and Hebi require significant VOC emission reductions. The value we recommended, here, is the median value of the 2+26 cities (black dots in Figure 4), and the ratio for few cities with higher control requirements will decrease as the joint air pollution control area is likely to expand in the future. Such results imply the strong seasonality of the optimized VOC/NO_x ratio that needs to be considered during policy making.

In the future, with decreasing precursor emissions, the VOC-sensitive regime, which requires synergistic VOC and NO_x controls, may transfer to a NO_x-sensitive regime.[56] Therefore, we determined the peak ratio (PR),[28,57] which is a robust responsive indicator for O_3 chemistry and is defined as the NO_x emission ratio at the peak pollutant concentrations under baseline VOC emissions (Figure 3b). Figure 4b also presents the PR values for the 2+26 cities for each month. The results show that in the winter (January, February, November, and December), when NO_x emission reduction exceeds 36−53% (median value of the 2+26 cities), the effect of VOC reduction is less than that of NO_x reduction. From May to September, the largest PR value was 45%. With the NO_x control, the regime will quickly transform to a NO_x-sensitive regime in the summer. Figure 4 suggests that similar emission reduction levels of VOCs and NO_x could prevent the increase in both $PM_{2.5}$ and O_3 concentrations, and simultaneous VOC controls are only needed until NO_x is reduced by less than 54% (the maximum average value of 2+26 cities in 12 months). The implementation of such an emission reduction path is more flexible, and it reflects the importance of coordinated VOC emission control in the short term and the necessity of large NO_x emission reduction in the long term. Compared to previous studies that employed high VOC emission reduction ratios to reduce O_3, this study proposed a comitigation pathway for $PM_{2.5}$ and O_3 by considering the dynamic changes in the atmospheric chemistry, rather than focusing solely on the immediate reduction.

Furthermore, note that it is hard to follow the exactly designed control ratio and pathway in reality. Thus, we suggested a priority control order of sectors based on the emissions. In the 2+26 cities, the NO_x and VOC emissions by industries, power plants, domestic sources, and transportation were 1.8 and 2.8, 0.6 and 0.0, 0.1 and 0.6, and 1.3 and 0.8 Mt, respectively. According to the total emissions of the sectors and the relative amounts of VOC and NO_x, the industrial and domestic sources can be controlled at the beginning stage to meet the minimum requirements of the VOC/NO_x ratio.

DISCUSSION

This study aimed to address the challenges facing China regarding air quality improvement, namely, the simultaneous reduction of $PM_{2.5}$ and O_3.

First, we assessed the reduction requirements for NO_x and VOCs to meet the air quality standard. Our results reveal that although the reduction of the emissions of NO_x by 81%, primary $PM_{2.5}$ by 65−87%, SO_2 by 49−85%, and NH_3 by 29% may cause the $PM_{2.5}$ and O_3 levels in the 2+26 cities to meet the NAAQS, such a strategy that does not control VOCs will cause huge losses of clean air benefits. A synergistic strategy for controlling VOCs and NO_x will afford substantial benefits to human health and crop production. Moreover, the benefits will increase with quicker implementations of the VOC emission reductions. The VOC emission reduction of 50% within 5 years, compared to the same reduction rate within 18 years, will afford benefits of ∼233 billion CHY.

Additionally, we determined that a wiser dual-pollutant control strategy is to strengthen VOCs and NO_x controls in the winter and summer, respectively. The current air pollution control policy in China, which emphasizes NO_x control in the winter, has been proven to be inefficient in reducing $PM_{2.5}$ and O_3 pollution in the last 5 years.[5,50] Our results suggest that similar VOC and NO_x emission control levels (i.e., a VOC/NO_x control ratio of 0.95 in December) are more effective in reducing the $PM_{2.5}$ concentrations in the winter. In the summer, the NO_x-sensitive regime for O_3 pollution requires enhanced NO_x emission control in addition to the current seasonal VOC control measures. These findings highlight the right pathways for future policy making to comitigate $PM_{2.5}$ and O_3 pollution in China and other countries.

This study has a few limitations. The uncertainty of the formation mechanism of secondary species (e.g., nitrate, sulfate, and OM) in the current model[58,59] will inevitably be introduced into the results. Similar to most previous modeling studies,[60] this study used the meteorological condition in a typical year (i.e., 2017) and focused on the control effectiveness under the fixed meteorological condition. The control effectiveness may vary with the changes in meteorological conditions;[61] however, studies have shown that the impact of emissions is more important in long-term than short-term variations,[9,62,63] and the substantial emission reductions could afford significantly improved air quality that could overwhelm the influences of future meteorology changes in the context of the carbon neutrality target.[64] Moreover, the meteorological condition in 2017 was considered as normal without specific climate events.[65] Further analysis on the impacts of changes in meteorological conditions on the relationship between emission and pollutant concentrations is recommended. For simplification, we applied a uniform reduction ratio for all VOC species, while priority was given to VOC species or sectors with larger contributions to $PM_{2.5}$ and O_3 pollution. Additionally, improved understanding of biogenic sources[66] will help improve the perception of anthropogenic emissions control. Since both $PM_{2.5}$ and O_3 are regional pollutants experiencing large influences from long-range transport,[67,68] it is impossible to achieve air targets by reducing the local emissions, particularly for cities in the border control regions (i.e., Tangshan, Taiyuan, Zibo, and Zhengzhou). Moreover, enlarging the coordinated areas to control emissions outside the 2+26 cities is also necessary. Here, we proposed the control strategy by considering air quality improvement and related benefits. In the future, the implementation feasibility of actual control measures should be analyzed.

Nevertheless, the clean air strategy, novel methods, and valuable insights proposed herein can be useful for China and

https://doi.org/10.1021/acs.est.1c04201
Environ. Sci. Technol. XXXX, XXX, XXX−XXX

all other countries facing air pollution issues for optimizing $PM_{2.5}$ and O_3 controls.

■ ASSOCIATED CONTENT

Supporting Information

The Supporting Information is available free of charge at https://pubs.acs.org/doi/10.1021/acs.est.1c04201.

> Simulation domain, major air pollutant emissions, validation of WRF and CMAQ simulations, validation of the response surface model prediction, contributions of inner-regional and outer-regional sources to $PM_{2.5}$ and O_3, impact of the size of the control area on the VOC/NO_x reduction requirement, NO_3^- and OM responded to the emission changes of NO_x and VOCs, crop yields and AOT40-yield response functions, and precursor emission ratio of the CBE scenario (PDF)

■ AUTHOR INFORMATION

Corresponding Authors

Jia Xing − *State Key Joint Laboratory of Environmental Simulation and Pollution Control, School of Environment, Tsinghua University, Beijing 100084, China; State Environmental Protection Key Laboratory of Sources and Control of Air Pollution Complex, Beijing 100084, China;* orcid.org/0000-0002-3716-8646; Email: xingjia@tsinghua.edu.cn

Shuxiao Wang − *State Key Joint Laboratory of Environmental Simulation and Pollution Control, School of Environment, Tsinghua University, Beijing 100084, China; State Environmental Protection Key Laboratory of Sources and Control of Air Pollution Complex, Beijing 100084, China;* orcid.org/0000-0001-9727-1963; Email: shxwang@tsinghua.edu.cn

Authors

Dian Ding − *State Key Joint Laboratory of Environmental Simulation and Pollution Control, School of Environment, Tsinghua University, Beijing 100084, China; Institute for Atmospheric and Earth System Research/Physics, Faculty of Science, University of Helsinki, 00014 Helsinki, Finland*

Zhaoxin Dong − *State Key Joint Laboratory of Environmental Simulation and Pollution Control, School of Environment, Tsinghua University, Beijing 100084, China*

Fenfen Zhang − *State Key Joint Laboratory of Environmental Simulation and Pollution Control, School of Environment, Tsinghua University, Beijing 100084, China*

Shuchang Liu − *State Key Joint Laboratory of Environmental Simulation and Pollution Control, School of Environment, Tsinghua University, Beijing 100084, China*

Jiming Hao − *State Key Joint Laboratory of Environmental Simulation and Pollution Control, School of Environment, Tsinghua University, Beijing 100084, China; State Environmental Protection Key Laboratory of Sources and Control of Air Pollution Complex, Beijing 100084, China*

Complete contact information is available at: https://pubs.acs.org/10.1021/acs.est.1c04201

Notes

The authors declare no competing financial interest.

■ ACKNOWLEDGMENTS

This work was supported by the National Natural Science Foundation of China (21625701 and 92044302), the Beijing Municipal Science and Technology Commission (Z191100009119004 and Z191100009119001), and the Tsinghua-Toyota Joint Research Institute Inter-Disciplinary Project. S.W. thanks the support of the Tencent Foundation through the XPLORER PRIZE. This work was completed on the "Explorer 100" cluster system of Tsinghua National Laboratory for Information Science and Technology.

■ REFERENCES

(1) Lu, X.; Zhang, S.; Xing, J.; Wang, Y.; Chen, W.; Ding, D.; Wu, Y.; Wang, S.; Duan, L.; Hao, J. Progress of Air Pollution Control in China and Its Challenges and Opportunities in the Ecological Civilization Era. *Engineering* **2020**, *6*, 1423−1431.

(2) Ding, D.; Xing, J.; Wang, S. X.; Liu, K. Y.; Hao, J. M. Estimated Contributions of Emissions Controls, Meteorological Factors, Population Growth, and Changes in Baseline Mortality to Reductions in Ambient PM2.5 and PM2.5-Related Mortality in China, 2013−2017. *Environ. Health Perspect.* **2019**, *127*, No. 067009.

(3) Xing, J.; Lu, X.; Wang, S.; Wang, T.; Ding, D.; Yu, S.; Shindell, D.; Ou, Y.; Morawska, L.; Li, S.; Ren, L.; Zhang, Y.; Loughlin, D.; Zheng, H.; Zhao, B.; Liu, S.; Smith, K. R.; Hao, J. The quest for improved air quality may push China to continue its its CO2 reduction beyond the Paris Commitment. *Proc. Natl. Acad. Sci. U.S.A.* **2020**, *117*, 29535−29542.

(4) *China Ecological Environment Status Bulletin*; China Ministry of Ecological Environment, 2017.

(5) Li, K.; Jacob, D.; Liao, H.; Zhu, J.; Shah, V.; Shen, L.; Bates, K.; Zhang, Q.; Zhai, S. A two-pollutant strategy for improving ozone and particulate air quality in China. *Nat. Geosci.* **2019**, *12*, 906−910.

(6) Xing, J.; Mathur, R.; Pleim, J.; Hogrefe, C.; Gan, C. M.; Wong, D. C.; Wei, C.; Wang, J. D. Air pollution and climate response to aerosol direct radiative effects: A modeling study of decadal trends across the northern hemisphere. *J. Geophys. Res.* **2015**, *120*, 12221−12236.

(7) Meng, Z.; Dabdub, D.; Seinfeld, J. H. Chemical coupling between atmospheric ozone and particulate matter. *Science* **1997**, *277*, 116−119.

(8) Li, K.; Jacob, D. J.; Liao, H.; Shen, L.; Zhang, Q.; Bates, K. H. Anthropogenic drivers of 2013-2017 trends in summer surface ozone in China. *Proc. Natl. Acad. Sci. U.S.A.* **2019**, *116*, 422−427.

(9) Ma, Z.; Xu, J.; Quan, W.; Zhang, Z.; Lin, W.; Xu, X. Significant increase of surface ozone at a rural site, north of eastern China. *Atmos. Chem. Phys.* **2016**, *16*, 3969−3977.

(10) Zheng, B.; Tong, D.; Li, M.; Liu, F.; Hong, C.; Geng, G.; Li, H.; Li, X.; Peng, L.; Qi, J.; Yan, L.; Zhang, Y.; Zhao, H.; Zheng, Y.; He, K.; Zhang, Q. Trends in China's anthropogenic emissions since 2010 as the consequence of clean air actions. *Atmos. Chem. Phys.* **2018**, *18*, 14095−14111.

(11) Lyu, X.; Wang, N.; Guo, H.; Xue, L.; Jiang, F.; Zeren, Y.; Cheng, H.; Cai, Z.; Han, L.; Zhou, Y. Causes of a continuous summertime O3 pollution event in Jinan, a central city in the North China Plain. *Atmos. Chem. Phys.* **2019**, *19*, 3025−3042.

(12) Yang, G.; Liu, Y.; Li, X. Spatiotemporal distribution of ground-level ozone in China at a city level. *Sci. Rep.* **2020**, *10*, No. 7229.

(13) Wang, N.; Lyu, X.; Deng, X.; Huang, X.; Jiang, F.; Ding, A. Aggravating O3 pollution due to NOx emission control in eastern China. *Sci. Total Environ.* **2019**, *677*, 732−744.

(14) Li, Y.; Lau, A. K. H.; Fung, J. C. H.; Zheng, J.; Liu, S. Importance of NOx control for peak ozone reduction in the Pearl River Delta region. *J. Geophys. Res.* **2013**, *118*, 9428−9443.

(15) Wang, X.; Fu, T.-M.; Zhang, L.; Cao, H.; Zhang, Q.; Ma, H.; Shen, L.; Evans, M. J.; Ivatt, P. D.; Lu, X.; Chen, Y.; Zhang, L.; Feng, X.; Yang, X.; Zhu, L.; Henze, D. K. Sensitivities of Ozone Air Pollution in the Beijing−Tianjin−Hebei Area to Local and Upwind

Precursor Emissions Using Adjoint Modeling. *Environ. Sci. Technol.* **2021**, *55*, 5752−5762.
(16) Xing, J.; Ding, D.; Wang, S.; Zhao, B.; Jang, C.; Wu, W.; Zhang, F.; Zhu, Y.; Hao, J. Quantification of the enhanced effectiveness of NOx control from simultaneous reductions of VOC and NH3 for reducing air pollution in the Beijing-Tianjin-Hebei region, China. *Atmos. Chem. Phys.* **2018**, *18*, 7799−7814.
(17) Chen, X.; Situ, S.; Zhang, Q.; Wang, X.; Sha, C.; Zhouc, L.; Wu, L.; Wu, L.; Ye, L.; Li, C. The synergetic control of NO2 and O3 concentrations in a manufacturing city of southern China. *Atmos. Environ.* **2019**, *201*, 402−416.
(18) Liu, H.; Wang, X.; Pang, J.; He, K. Feasibility and difficulties on China new air quality standard compliance: PRD case of PM2.5 and ozone from 2010 to 2025. *Atmos. Chem. Phys.* **2013**, *13*, 12013−12027.
(19) Liu, Z.; Qi, Z.; Ni, X.; Dong, M.; Ma, M.; Xue, W.; Zhang, Q.; Wang, J. How to apply O3 and PM2.5 collaborative control to practical management in China: A study based on meta-analysis and machine learning. *Sci. Total Environ.* **2021**, *772*, No. 145392.
(20) Xiang, S.; Liu, J.; Tao, W.; Kan, Y.; Xu, J.; Hu, X.; Liu, H.; Wang, Y.; Zhang, Y.; Yang, H.; Hu, J.; Wan, Y.; Wang, X.; Ma, J.; Wang, X.; Tao, S. Control of both PM2.5 and O3 in Beijing-Tianjin-Hebei and the surrounding areas. *Atmos. Environ.* **2020**, *224*, No. 117259.
(21) Appel, W.; Napelenok, S.; Hogrefe, C.; Pouliot, G.; Foley, K. M.; Roselle, S. J.; Pleim, J. E.; Bash, J.; Pye, H. O. T.; Heath, N.; Murphy, B.; Mathur, R. Overview and Evaluation of the Community Multiscale Air Quality (CMAQ) Modeling System Version 5.2. In *Air Pollution Modeling and Its Application XXV*; Springer International Publishing AG: Cham (ZG), Switzerland, 2018; pp 69−73.
(22) Sarwar, G.; Luecken, D.; Yarwood, G.; Whitten, G. Z.; Carter, W. P. L. Impact of an updated carbon bond mechanism on predictions from the CMAQ modeling system: Preliminary assessment. *J. Appl. Meteorol. Climatol.* **2008**, *47*, 3−14.
(23) Appel, K. W.; Pouliot, G. A.; Simon, H.; Sarwar, G.; Pye, H. O. T.; Napelenok, S. L.; Akhtar, F.; Roselle, S. J. Evaluation of dust and trace metal estimates from the Community Multiscale Air Quality (CMAQ) model version 5.0. *Geosci. Model Dev.* **2013**, *6*, 883−899.
(24) Li, M.; Zhang, Q.; Kurokawa, J.-i.; Woo, J.-H.; He, K.; Lu, Z.; Ohara, T.; Song, Y.; Streets, D. G.; Carmichael, G. R.; Cheng, Y.; Hong, C.; Huo, H.; Jiang, X.; Kang, S.; Liu, F.; Su, H.; Zheng, B. MIX: a mosaic Asian anthropogenic emission inventory under the international collaboration framework of the MICS-Asia and HTAP. *Atmos. Chem. Phys.* **2017**, *17*, 935−963.
(25) Guenther, A.; Karl, T.; Harley, P.; Wiedinmyer, C.; Palmer, P. I.; Geron, C. Estimates of global terrestrial isoprene emissions using MEGAN (Model of Emissions of Gases and Aerosols from Nature). *Atmos. Chem. Phys.* **2006**, *6*, 3181−3210.
(26) Skamarock, W. C.; Klemp, J. B.; Dudhia, J.; Gill, D. O.; Barker, D. M.; Duda, M. G.; Huang, X.-Y.; Wang, W.; Powers, J. G. *A Description of the Advanced Research WRF Version 3, NCAR Technical Note NCAR/TN-475+STR*; 2008.
(27) Wang, S.; Xing, J.; Jang, C.; Zhu, Y.; Fu, J. S.; Hao, J. Impact Assessment of Ammonia Emissions on Inorganic Aerosols in East China Using Response Surface Modeling Technique. *Environ. Sci. Technol.* **2011**, *45*, 9293−9300.
(28) Xing, J.; Wang, S. X.; Jang, C.; Zhu, Y.; Hao, J. M. Nonlinear response of ozone to precursor emission changes in China: a modeling study using response surface methodology. *Atmos. Chem. Phys.* **2011**, *11*, 5027−5044.
(29) Zhao, B.; Wang, S. X.; Xing, J.; Fu, K.; Fu, J. S.; Jang, C.; Zhu, Y.; Dong, X. Y.; Gao, Y.; Wu, W. J.; Wang, J. D.; Hao, J. M. Assessing the nonlinear response of fine particles to precursor emissions: development and application of an extended response surface modeling technique v1.0. *Geosci. Model Dev.* **2015**, *8*, 115−128.
(30) Zhao, B.; Wu, W.; Wang, S.; Xing, J.; Chang, X.; Liou, K.-N.; Jiang, J. H.; Gu, Y.; Jang, C.; Fu, J. S.; Zhu, Y.; Wang, J.; Lin, Y.; Hao, J. A modeling study of the nonlinear response of fine particles to air pollutant emissions in the Beijing-Tianjin-Hebei region. *Atmos. Chem. Phys.* **2017**, *17*, 12031−12050.
(31) Xing, J.; Wang, S.; Zhao, B.; Wu, W.; Ding, D.; Jang, C.; Zhu, Y.; Chang, X.; Wang, J.; Zhang, F.; Hao, J. Quantifying Nonlinear Multiregional Contributions to Ozone and Fine Particles Using an Updated Response Surface Modeling Technique. *Environ. Sci. Technol.* **2017**, *51*, 11788−11798.
(32) Xing, J.; Ding, D.; Wang, S.; Zhao, B.; Jang, C.; Wu, W.; Zhang, F.; Zhu, Y.; Hao, J. Quantification of the enhanced effectiveness of NOx control from simultaneous reductions of VOC and NH3 for reducing air pollution in the Beijing−Tianjin−Hebei region, China. *Atmos. Chem. Phys.* **2018**, *18*, 7799−7814.
(33) Xing, J.; Zhang, F.; Zhou, Y.; Wang, S.; Ding, D.; Jang, C.; Zhu, Y.; Hao, J. Least-cost control strategy optimization for air quality attainment of Beijing−Tianjin−Hebei region in China. *J. Environ. Manage.* **2019**, *245*, 95−104.
(34) Li, T.; Zhang, Y.; Wang, J.; Xu, D.; Yin, Z.; Chen, H.; Lv, Y.; Luo, J.; Zeng, Y.; Liu, Y.; Kinney, P. L.; Shi, X. All-cause mortality risk associated with long-term exposure to ambient PM2.5 in China: a cohort study. *Lancet Public Health* **2018**, *3*, E470−E477.
(35) Burnett, R.; Chen, H.; Szyszkowicz, M.; Fann, N.; Hubbell, B.; Pope, C. A.; Apte, J. S.; Brauer, M.; Cohen, A.; Weichenthal, S.; Coggins, J.; Di, Q.; Brunekreef, B.; Frostad, J.; Lim, S. S.; Kan, H.; Walker, K. D.; Thurston, G. D.; Hayes, R. B.; Lim, C. C.; Turner, M. C.; Jerrett, M.; Krewski, D.; Gapstur, S. M.; Diver, W. R.; Ostro, B.; Goldberg, D.; Crouse, D. L.; Martin, R. V.; Peters, P.; Pinault, L.; Tjepkema, M.; van Donkelaar, A.; Villeneuve, P. J.; Miller, A. B.; Yin, P.; Zhou, M.; Wang, L.; Janssen, N. A. H.; Marra, M.; Atkinson, R. W.; Tsang, H.; Quoc Thach, T.; Cannon, J. B.; Allen, R. T.; Hart, J. E.; Laden, F.; Cesaroni, G.; Forastiere, F.; Weinmayr, G.; Jaensch, A.; Nagel, G.; Concin, H.; Spadaro, J. V. Global estimates of mortality associated with long-term exposure to outdoor fine particulate matter. *Proc. Natl. Acad. Sci. U.S.A.* **2018**, *115*, 9592.
(36) Yin, P.; Brauer, M.; Cohen, A.; Burnett Richard, T.; Liu, J.; Liu, Y.; Liang, R.; Wang, W.; Qi, J.; Wang, L.; Zhou, M. Long-term Fine Particulate Matter Exposure and Nonaccidental and Cause-specific Mortality in a Large National Cohort of Chinese Men. *Environ. Health Perspect.* **2017**, *125*, No. 117002.
(37) Global Burden of Disease Collaborative Network. *Global Burden of Disease Study 2017 (GBD 2017) Results*; Institute for Health Metrics and Evaluation (IHME): Seattle, 2018; http://ghdx.healthdata.org/gbd-results-tool.
(38) *China Statistical Yearbook 2018*; National Bureau of Statistics of China, 2018.
(39) Turner, M. C.; Jerrett, M.; Pope, C. A.; Krewski, D.; Gapstur, S. M.; Diver, W. R.; Beckerman, B. S.; Marshall, J. D.; Su, J.; Crouse, D. L.; Burnett, R. T. Long-Term Ozone Exposure and Mortality in a Large Prospective Study. *Am. J. Respir. Crit. Care Med.* **2016**, *193*, 1134−1142.
(40) Huang, D.; Andersson, H.; Zhang, S. Willingness to pay to reduce health risks related to air quality: evidence from a choice experiment survey in Beijing. *J. Environ. Planning Manage.* **2018**, *61*, 2207−2229.
(41) Feng, Z.; De Marco, A.; Anav, A.; Gualtieri, M.; Sicard, P.; Tian, H.; Fornasier, F.; Tao, F.; Guo, A.; Paoletti, E. Economic losses due to ozone impacts on human health, forest productivity and crop yield across China. *Environ. Int.* **2019**, *131*, No. 104966.
(42) Peng, J.; Shang, B.; Xu, Y.; Feng, Z.; Pleijel, H.; Calatayud, V. Ozone exposure- and flux-yield response relationships for maize. *Environ. Pollut.* **2019**, *252*, 1−7.
(43) Zhao, H.; Zheng, Y.; Zhang, Y.; Li, T. Evaluating the effects of surface O3 on three main food crops across China during 2015−2018. *Environ. Pollut.* **2020**, *258*, No. 113794.
(44) Zhao, B.; Wang, S.; Ding, D.; Wu, W.; Chang, X.; Wang, J.; Xing, J.; Jang, C.; Fu, J. S.; Zhu, Y.; et al. Nonlinear relationships between air pollutant emissions and PM2.5-related health impacts in the Beijing-Tianjin-Hebei region. *Sci. Total Environ.* **2019**, *661*, 375−385.

https://doi.org/10.1021/acs.est.1c04201
Environ. Sci. Technol. XXXX, XXX, XXX−XXX

(45) Anger, A.; Dessens, O.; Xi, F.; Barker, T.; Wu, R. China's air pollution reduction efforts may result in an increase in surface ozone levels in highly polluted areas. *Ambio* **2016**, *45*, 254−265.
(46) Zhao, Y.; Zhang, K.; Xu, X.; Shen, H.; Zhu, X.; Zhang, Y.; Hu, Y.; Shen, G. Substantial Changes in Nitrogen Dioxide and Ozone after Excluding Meteorological Impacts during the COVID-19 Outbreak in Mainland China. *Environ. Sci. Technol. Lett.* **2020**, *7*, 402−408.
(47) Sicard, P.; De Marco, A.; Agathokleous, E.; Feng, Z.; Xu, X.; Paoletti, E.; Rodriguez, J. J. D.; Calatayud, V. Amplified ozone pollution in cities during the COVID-19 lockdown. *Sci. Total Environ.* **2020**, *735*, No. 139542.
(48) Miyazaki, K.; Bowman, K.; Sekiya, T.; Jiang, Z.; Chen, X.; Eskes, H.; Ru, M.; Zhang, Y.; Shindell, D. Air Quality Response in China Linked to the 2019 Novel Coronavirus (COVID-19) Lockdown. *Geophys. Res. Lett.* **2020**, *47*, No. e2020GL089252.
(49) Le, T.; Wang, Y.; Liu, L.; Yang, J.; Yung, Y. L.; Li, G.; Seinfeld, J. H. Unexpected air pollution with marked emission reductions during the COVID-19 outbreak in China. *Science* **2020**, *369*, 702.
(50) Leung, D. M.; Shi, H.; Zhao, B.; Wang, J.; Ding, E. M.; Gu, Y.; Zheng, H.; Chen, G.; Liou, K.-N.; Wang, S.; Fast, J. D.; Zheng, G.; Jiang, J.; Li, X.; Jiang, J. H. Wintertime Particulate Matter Decrease Buffered by Unfavorable Chemical Processes Despite Emissions Reductions in China. *Geophys. Res. Lett.* **2020**, *47*, No. e2020GL087721.
(51) Huang, X.; Ding, A.; Gao, J.; Zheng, B.; Zhou, D.; Qi, X.; Tang, R.; Wang, J.; Ren, C.; Nie, W.; Chi, X.; Xu, Z.; Chen, L.; Li, Y.; Che, F.; Pang, N.; Wang, H.; Tong, D.; Qin, W.; Cheng, W.; Liu, W.; Fu, Q.; Liu, B.; Chai, F.; Davis, S. J.; Zhang, Q.; He, K. Enhanced secondary pollution offset reduction of primary emissions during COVID-19 lockdown in China. *Natl. Sci. Rev.* **2021**, *8*, No. nwaa137.
(52) Fu, X.; Wang, T.; Gao, J.; Wang, P.; Liu, Y.; Wang, S.; Zhao, B.; Xue, L. Persistent Heavy Winter Nitrate Pollution Driven by Increased Photochemical Oxidants in Northern China. *Environ. Sci. Technol.* **2020**, *54*, 3881−3889.
(53) Kang, M.; Zhang, J.; Zhang, H.; Ying, Q. On the Relevancy of Observed Ozone Increase during COVID-19 Lockdown to Summertime Ozone and PM2.5 Control Policies in China. *Environ. Sci. Technol. Lett.* **2021**, *8*, 289−294.
(54) Lin, H.; Wang, M.; Duan, Y.; Fu, Q.; Ji, W.; Cui, H.; Jin, D.; Lin, Y.; Hu, K. O3 Sensitivity and Contributions of Different NMHC Sources in O3 Formation at Urban and Suburban Sites in Shanghai. *Atmosphere* **2020**, *11*, No. 295.
(55) Lu, H.; Lyu, X.; Cheng, H.; Ling, Z.; Guo, H. Overview on the spatial-temporal characteristics of the ozone formation regime in China. *Environ. Sci. Processes Impacts* **2019**, *21*, 916−929.
(56) Souri, A. H.; Nowlan, C. R.; González Abad, G.; Zhu, L.; Blake, D. R.; Fried, A.; Weinheimer, A. J.; Wisthaler, A.; Woo, J. H.; Zhang, Q.; Chan Miller, C. E.; Liu, X.; Chance, K. An inversion of NOx and non-methane volatile organic compound (NMVOC) emissions using satellite observations during the KORUS-AQ campaign and implications for surface ozone over East Asia. *Atmos. Chem. Phys.* **2020**, *20*, 9837−9854.
(57) Xing, J.; Ding, D.; Wang, S.; Dong, Z.; Kelly, J. T.; Jang, C.; Zhu, Y.; Hao, J. Development and application of observable response indicators for design of an effective ozone and fine particle pollution control strategy in China. *Atmos. Chem. Phys.* **2019**, *19*, 13627−13646.
(58) Zheng, H.; Song, S.; Sarwar, G.; Gen, M.; Wang, S.; Ding, D.; Chang, X.; Zhang, S.; Xing, J.; Sun, Y.; Ji, D.; Chan, C. K.; Gao, J.; McElroy, M. B. Contribution of Particulate Nitrate Photolysis to Heterogeneous Sulfate Formation for Winter Haze in China. *Environ. Sci. Technol. Lett.* **2020**, *7*, 632−638.
(59) Zhang, J.; Choi, M.; Ji, Y.; Zhang, R.; Zhang, R.; Ying, Q. Assessing the Uncertainties in Ozone and SOA Predictions due to Different Branching Ratios of the Cresol Pathway in the Toluene-OH Oxidation Mechanism. *ACS Earth Space Chem.* **2021**, *5*, 1958−1970.
(60) Tong, D.; Geng, G.; Jiang, K.; Cheng, J.; Zheng, Y.; Hong, C.; Yan, L.; Zhang, Y.; Chen, X.; Bo, Y.; Lei, Y.; Zhang, Q.; He, K. Energy and emission pathways towards PM2.5 air quality attainment in the Beijing-Tianjin-Hebei region by 2030. *Sci. Total Environ.* **2019**, *692*, 361−370.
(61) Liu, Y.; Wang, T. Worsening urban ozone pollution in China from 2013 to 2017 − Part 1: The complex and varying roles of meteorology. *Atmos. Chem. Phys.* **2020**, *20*, 6305−6321.
(62) Xu, Y.; Xue, W.; Lei, Y.; Huang, Q.; Zhao, Y.; Cheng, S.; Ren, Z.; Wang, J. Spatiotemporal variation in the impact of meteorological conditions on PM2.5 pollution in China from 2000 to 2017. *Atmos. Environ.* **2019**, *223*, No. 117215.
(63) Li, K.; Jacob, D. J.; Shen, L.; Lu, X.; De Smedt, I.; Liao, H. Increases in surface ozone pollution in China from 2013 to 2019: anthropogenic and meteorological influences. *Atmos. Chem. Phys.* **2020**, *20*, 11423−11433.
(64) Liu, S.; Xing, J.; Wang, S.; Ding, D.; Cui, Y.; Hao, J. Health Benefits of Emission Reduction under 1.5 °C Pathways Far Outweigh Climate-Related Variations in China. *Environ. Sci. Technol.* **2021**, *55*, 10957−10966.
(65) Feng, A.; Zeng, H.; Yin, Y.; Song, Y.; Liu, Y.; Wang, Y.; Wang, L.; Wang, Y.; Zhu, X.; Cai, W.; Hou, W.; Huang, D.; Guo, Y.; Zhang, Y.; Zhong, H.; Li, Y.; Shi, S.; Zhi, R.; Hong, J.; Wang, D. Climatic Characteristics and Major Meteorological Events over China in 2017. *Meteorol. Mon.* **2018**, *44*, 548−555.
(66) Lu, X.; Ye, X.; Zhou, M.; Zhao, Y.; Weng, H.; Kong, H.; Li, K.; Gao, M.; Zheng, B.; Lin, J.; Zhou, F.; Zhang, Q.; Wu, D.; Zhang, L.; Zhang, Y. The underappreciated role of agricultural soil nitrogen oxide emissions in ozone pollution regulation in North China. *Nat. Commun.* **2021**, *12*, No. 5021.
(67) Chang, X.; Wang, S.; Zhao, B.; Xing, J.; Liu, X.; Wei, L.; Song, Y.; Wu, W.; Cai, S.; Zheng, H.; Ding, D.; Zheng, M. Contributions of inter-city and regional transport to PM2.5 concentrations in the Beijing-Tianjin-Hebei region and its implications on regional joint air pollution control. *Sci. Total Environ.* **2019**, *660*, 1191−1200.
(68) Dong, Z.; Wang, S.; Xing, J.; Chang, X.; Ding, D.; Zheng, H. Regional transport in Beijing-Tianjin-Hebei region and its changes during 2014−2017: The impacts of meteorology and emission reduction. *Sci. Total Environ.* **2020**, *737*, No. 139792.

https://doi.org/10.1021/acs.est.1c04201
Environ. Sci. Technol. XXXX, XXX, XXX−XXX